



CrossMark
click for updates

Cite this: *RSC Adv.*, 2016, 6, 15354

Highly selective one-step hydrogenation of nitrobenzene to cyclohexylamine over the supported 10% Ni/carbon catalysts doped with 3% Rh[†]

Xinhuan Lu,^{abc} Yang chen,^{ac} Zhenshuang Zhao,^{ac} Hao Deng,^{ac} Dan Zhou,^{*ac} Changcheng Wei,^{ac} Renfeng Nie^{ac} and Qinghua Xia^{*ac}

The carbon supported 10% Ni catalysts doped with 3% Rh have been prepared by an impregnation method. These catalysts have been used to catalyze the one-step hydrogenation of nitrobenzene to cyclohexylamine. The results show that the 3% Rh–10% Ni/CSC (biocarbon) catalyst exhibits an excellent performance to achieve 100 mol% conversion of nitrobenzene and 91.6% selectivity of cyclohexylamine under reaction conditions of 3.5 MPa and 140 °C. The recycling tests reveal recyclable stability of 3% Rh–10% Ni/CSC. This catalyst is active for the hydrogenation of a series of electron-deficient nitrobenzenes. Some factors such as the type of carriers, the content of Ni and Rh, the type of metals and additives play important roles in controlling the selective hydrogenation.

Received 26th December 2015

Accepted 27th January 2016

DOI: 10.1039/c5ra27202e

www.rsc.org/advances

1. Introduction

Cycloaliphatic amines are one kind of important organic chemical and fine chemical intermediate, and also an important raw material for the synthesis of isocyanate. The hydrogenation of aromatic amines is the most commonly used method for the synthesis of cycloaliphatic amines.^{1–3} The catalytic hydrogenation of nitroaromatic compounds to the corresponding anilines is an important process for the production of many fine chemicals, such as dyes, drugs, herbicides, cosmetics, and pesticides.^{4,5} However, it is not easy to avoid the occurrence of dehalogenation during reactions.^{6,7} The hydrogenation of aniline over transition metal catalysts is accompanied by numerous side reactions. In addition to cyclohexylamine (CHA), the products always include dicyclohexylamine (DCHA) and ammonia. At elevated temperature, the formation of diphenylamine, phenyl-cyclohexylamine, cyclohexane and benzene is also reported.⁸ Moreover, in aqueous media, hydrolytic products like cyclohexanone and cyclohexanol could also be detected.^{9,10}

Cyclohexylamine can be used in the synthesis of artificial sweeteners (sodium or calcium cyclamate), metal corrosion inhibitors, rubber vulcanizing additives, dyestuff, plasticizers and extracting agents for natural products.^{11–13} Industrially, CHA is produced *via* the following two steps, (i) the reduction of nitrobenzene (NB) to aniline,^{14–20} (ii) the ring hydrogenation of aniline to CHA,^{21–26} which is a complicated process. More importantly, the selectivity of cyclohexylamine is low only in the range of 30–50%. Therefore, the development of a facile ‘one-step’ synthetic pathway from nitroarenes to alicyclic amines is of great importance.

Transition-metal nanoparticles as catalysts have attracted much attention due to the fact that if controlled, their surface structures often give rise to high chemo-, regio-, stereo- and enantio- selectivities.^{27–33} As to the industrial process to manufacture aniline through the hydrogenation of nitrobenzene, it is generally run above 240 °C with the copper catalyst in two-stage fixed-bed reactor.³⁴ In the hydrogenation of aniline in the vapor phase or in the liquid phase, the activity of a variety of metals such as Ni, Co, Rh, Ru, Pd or Pt has been studied as well.^{35–39} It is well known that Pt usually catalyzes a fast reduction of nitro group but with a low full-hydrogenation selectivity, and Ru is cheaper and more selective than other noble metals for this reaction but with a low catalytic activity.^{40,41} Recently, Langer *et al.* reported a low-pressure process for the hydrogenation of aniline to CHA with a high selectivity over rhodium (Rh) catalysts.⁴² This approach might provide a green pathway from the view point of efficiency.

Very recently, our group reported the ‘one-step’ catalytic hydrogenation from 1,5-dinitronaphthalene to 1,5-diamino

^aHubei Collaborative Innovation Center for Advanced Organic Chemical Materials, Hubei University, Wuhan 430062, P. R. China. E-mail: d.zhou@hubei.edu.cn; xiaqh518@aliyun.com; Fax: +86-27-88663043; Tel: +86-27-88663043

^bHubei Key Laboratory for Processing and Application of Catalytic Materials, Huanggang Normal University, Huanggang 438000, P. R. China

^cMinistry-of-Education Key Laboratory for the Synthesis and Application of Organic Functional Molecules, Hubei University, Wuhan 430062, P. R. China

[†] Electronic supplementary information (ESI) available. See DOI: 10.1039/c5ra27202e

decahydronaphthalene over the supported Ni catalysts,⁴³ which can completely skip the synthesis of aromatic amine intermediates. To date, only one report has approached the 'one-step' catalytic hydrogenation from nitrobenzene to cyclohexylamine over noble metal catalyst.⁴⁴ The present work describes a direct synthesis of alicyclic amines through the hydrogenation of nitroarenes with H₂ over carbon supported 10% Ni catalysts promoted with 3‰ Rh. The study is mainly focused on highly selective one-step hydrogenation from nitrobenzene to cyclohexylamine, for which the best data are 100 mol% conversion of nitrobenzene and 91.6% selectivity of cyclohexylamine under mild conditions.

2. Experimental

2.1. Materials

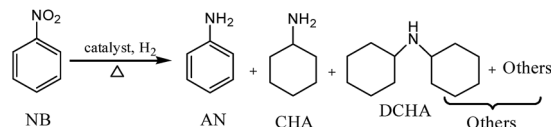
Raney Ni (99.5%), Ni(NO₃)₂·6H₂O (98%), RhCl₃·3H₂O (Rh 40%), PdCl₂ (Pd 59–60%), coconut shell charcoal (CSC) (98%), activated carbon (AC) (97%) and graphite (G) (97%) were purchased from Shanghai Aladdin Chemical Co. Note that CSC is made from high-quality coconut shell biomaterial, which has porous structure, large specific surface area, strong adsorption ability and easy regeneration. The main reagents used in the hydrogenations were nitrobenzene (99.0%), 2-nitrotoluene (98.0%), 3-methylnitrobenzene (98.0%), 4-methylnitrobenzene (99.0%), 2-chloronitrobenzene (98.0%), 3-chloronitrobenzene (98.0%) and 4-chloronitrobenzene (98.0%), methanol (99.0%), dioxane (99.0%), ethyl acetate (99.0%), tetrahydrofuran (THF) (99.0%) and cyclohexane (99.0%), which were purchased from Shanghai Aladdin Chemical Co. and directly used as received. The basic additives included LiOH (99.0%), NaNH₂ (99.5%), K₂CO₃ (99.0%) and NaHCO₃ (99.0%).

2.2. Preparation of catalysts

An aqueous solution of Ni(NO₃)₂·6H₂O or precious metal chlorides was impregnated onto various carbon supports like CSC, AC and G. The supported catalysts were prepared through the following procedure. Typically, 2.0 g of carbon material was dispersed into the solution consisted of Ni(NO₃)₂·6H₂O (0.098–1.480 g), RhCl₃·3H₂O (1.02 × 10⁻³ to 10.2 × 10⁻³ g) and distilled water (30 g). Then, the resulting mixture was heated to 80 °C while stirring until water was completely evaporated off. The solid was dried at 100 °C for 12 h, then calcined at 300–400 °C for 3 h in the flow of air, and reduced by hydrogen at 300–400 °C for 3 h in a tubular reactor. The resultant catalyst was designated as x% Ni/CSC, 3‰ Rh–x% Ni/CSC, x‰ Rh–10% Ni/CSC, 10% Ni/AC, 10% Ni/G, in which x% corresponds to 1–15% (mass percentage). Other carbon supported metal catalysts were prepared with a similar method, which was designated as, 10% Fe/CSC, 10% Cu/CSC, 10% Co/CSC and 10% Mo/CSC.

2.3. Characterization of catalysts

Powder X-ray diffraction (XRD) was performed on a Bruker D8A25 diffractometer with CuKα radiation (λ = 1.54184 Å) operating at 30 kV and 25 mA in the range of 5–65° 2θ.



Scheme 1 The hydrogenated products of nitrobenzene.

Autosorb-1 was used to determine N₂ adsorption–desorption properties of the samples. The Brunauer–Emmett–Teller (BET) specific surface area was calculated using the BET equation in the relative pressure between 0.05 and 0.25. The morphology and size of crystals were imaged with a JEOL JSM-6510A scanning electron microscope (SEM). Transmission electron microscope (TEM) images were obtained using an accelerating voltage of 200 kV on a JEOL-135 2010F transmission electron microscope. X-ray photoelectron spectra (XPS) were recorded on a Perkin-Elmer PHI ESCA system. X-ray source was standard Mg anode (1253.6 eV) at 12 kV and 300 W. The temperature programmed H₂ reduction (TPR) on a TP-5076 dynamic adsorption analyzer, which was carried out in a N₂ flow of 50 mL min⁻¹ (10 vol% H₂), from room temperature to 600 °C at a heating rate of 10 °C min⁻¹.

2.4. Catalytic tests

The catalytic hydrogenations of nitrobenzene (NB) to cyclohexylamine (CHA) were carried out in a 100 mL stainless autoclave. In a typical procedure, a certain amount of catalyst was dispersed in 9.0 g solvent, and then added with 1.0 g substrate. The autoclave was sealed, purged and pressurized with hydrogen, and then heated to desired temperature under magnetic stirring at a rate of 1000 rpm. After the completion of the reaction, the mixture was separated by centrifugation in order to recover the solid catalyst. Then, the solid catalyst was washed with acetone and dried in vacuum oven for the next use. The filtrate was analyzed by gas-chromatogram (GC, GC9720) with a 30 m capillary column (Rtx@-5) using a flame ionization detector (FID). The standard samples of cyclohexylamine and dicyclohexylamine were used as the reference of the GC retention time of hydrogenated products. As illustrated in Scheme 1, the hydrogenated products were mainly consisted of aniline (AN), cyclohexylamine (CHA), dicyclohexylamine (DCHA), and others (some cracked byproducts), GC-MS of which were shown in Fig. S1.†

3. Results and discussion

3.1. Structural characteristics of catalysts

Fig. 1 presents the XRD patterns of the samples with different Ni contents, in which weak peaks due to 1% Ni can be seen. The characteristic peaks of CSC (2θ = 23.3°) and Ni metal (2θ = 44.4 and 51.6°) are observed for all the Ni/CSC catalysts with the Ni loading from 3–15 wt%, in which two peaks at 44.4° and 51.6° are attributed to [111] and [200] diffraction peaks of NiO. This means that the crystalline structure of CSC was not yet destroyed and the Ni species were reduced to NiO metal in all the catalysts during the preparation. Moreover, with increasing

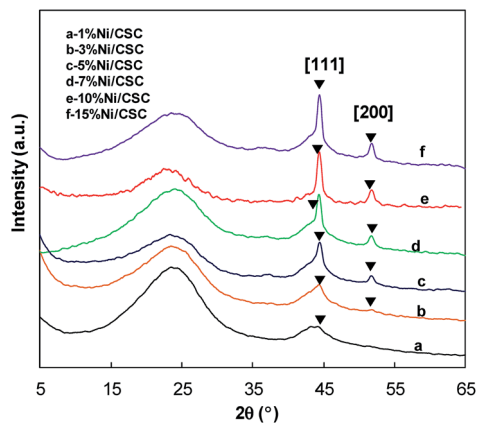


Fig. 1 XRD patterns of various Ni/CSC catalysts with different Ni contents.

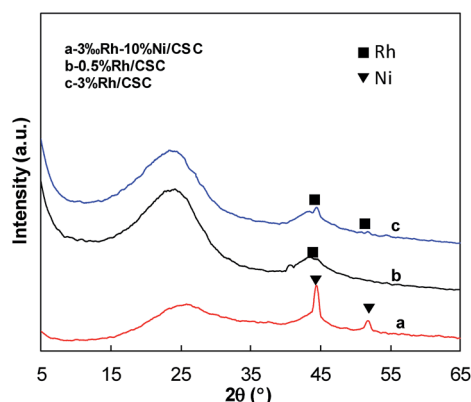


Fig. 2 XRD patterns of CSC supported Rh catalysts.

the Ni content, the intensity of [111] and [200] diffraction peaks is gradually increased. Fig. 2 shows the XRD patterns of CSC supported Rh catalysts. The Rh peak of 0.5% Rh/CSC is not obvious, showing that Rh particles are uniformly dispersed on the CSC carrier. There are two weak peaks visible at $2\theta = 43.2$ and 50.9° for 3% Rh/CSC, probably due to the formation of small Rh crystals on CSC. The Rh peak of 3% Rh-10% Ni/CSC is also not obvious, possibly because of low Rh content and the concealment of strong Ni peak.

The X-ray diffraction patterns of the samples of CSC supported other metals are shown in Fig. S2.† The peak located at 23.3° is characteristic of typical CSC material. The peaks at $2\theta = 37.6^\circ$ and 52.7° are ascribed to molybdenum oxide. The XRD peak of Fe metal appears at $2\theta = 45.2^\circ$, and the peaks at $2\theta = 30.8^\circ$, 42.6° , 53.0° , 56.6° and 63.5° are indexed to Fe_2O_3 . The above results show that the reduction temperature of 400°C is insufficient for the preparation of 10% Mo/CSC and 10% Fe/CSC catalysts. As can be seen from Fig. S2,† the peaks at 41.0° , 43.9° and 46.8° are attributed to Co metal, and ones at 42.8° and 51.1° correspond the crystalline phase of Cu on CSC, showing that Co or Cu oxides can be totally reduced at 400°C .

Table S1† presents the BET surface areas and total pore volumes of various catalysts determined by the BET analysis.

Very clearly, the support G and the catalyst 10% Ni/G has the smallest BET surface areas and pore volumes. Both values of the catalyst 10% Ni/AC (activated carbon as the support) are the largest. The increase of Ni content has led to a small drop of BET surface area and pore volume from $684.6\text{ m}^2\text{ g}^{-1}$ ($0.32\text{ cm}^3\text{ g}^{-1}$) of CSC to $673.8\text{ m}^2\text{ g}^{-1}$ ($0.29\text{ cm}^3\text{ g}^{-1}$) of 15% Ni/CSC. The BET surface area and pore volume of the catalyst 3% Rh/CSC are $678.9\text{ m}^2\text{ g}^{-1}$ and $0.31\text{ cm}^3\text{ g}^{-1}$.

Fig. S3† shows SEM images of CSC supported Ni or Rh catalysts, inclusive of CSC, 1% Ni/CSC, 3% Ni/CSC, 10% Ni/CSC, 15% Ni/CSC, 0.5% Rh/CSC, 3% Rh/CSC and 3% Rh-10% Ni/CSC. Apparently, SEM images of the latter six samples exhibit irregular spherical morphologies, different from fine particles of CSC, Ni and Rh components dispersed highly on the support. The sharp boundaries of the particles demonstrate crystalline characteristics of these samples, in which the particle shape and size of different catalysts are decided by the morphology of different carriers, further affecting catalytic activities. Fig. S4† shows the SEM images of CSC supported other metal catalysts, which exhibit irregular spherical morphologies.

Fig. 3 shows TEM images of CSC supported Ni or Rh catalysts. The TEM image of unreduced precursor NiO/CSC of 10% Ni/CSC shows very vague particle interface. Once reduced, the 10% Ni/CSC catalyst contains nanosized Ni particles, normally in the order of 5.1–33.1 nm, in which the average Ni particle size

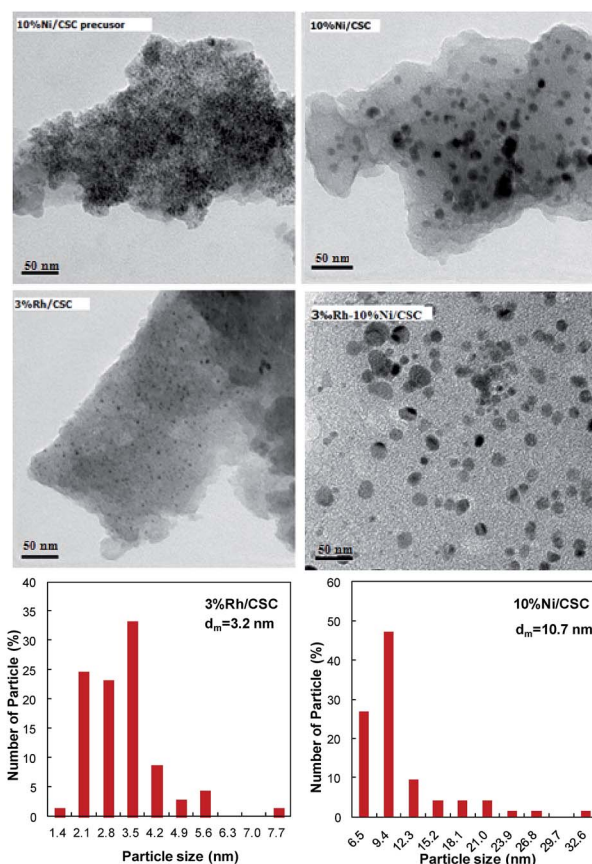


Fig. 3 TEM images of the supported catalysts and size distribution of Ni or Rh particles on 10% Ni/CSC and 3% Rh/CSC.

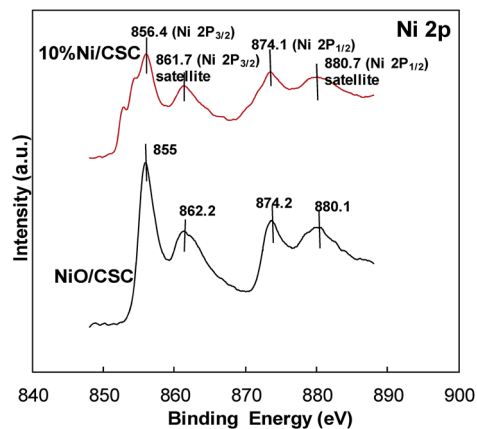


Fig. 4 Ni2p XPS spectra of NiO/CSC (precursor of 10% Ni/CSC) and 10% Ni/CSC.

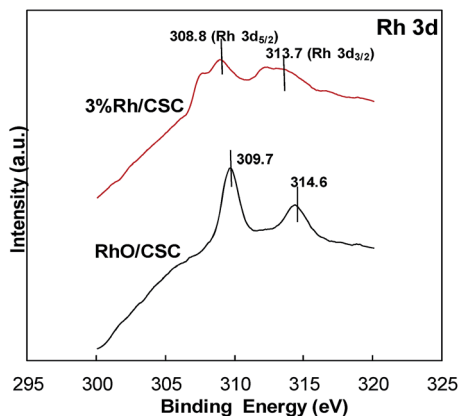


Fig. 5 Rh3d XPS spectra of RhO/CSC (precursor of 3% Rh/CSC) and 3% Rh/CSC.

is 10.7 nm. In addition, Rh nanoparticles on the CSC support are quite small with the mean particle size of 3.2 nm. The TEM image of 3% Rh–10% Ni/CSC composite catalyst looks similar to that of 10% Ni/CSC, in which Ni particles and Rh particles are visible. Fig. 4 shows the Ni2p XPS spectra of 10% Ni/CSC and the precursor NiO/CSC (unreduced). The peaks emerge at *ca.* 855 and 874.2 eV for NiO/CSC, ascribable to the Ni2p binding energy of Ni²⁺; however, after being reduced by H₂, those peaks shift to 856.4 and 874.1 eV, characteristic of Ni2p_{3/2} and Ni2p_{1/2} binding energies of metallic nickel.^{43,45} Fig. 5 shows the Rh3d XPS spectra of the sample 3% Rh/CSC and the precursor RhO_x/CSC (unreduced). The peaks emerge at *ca.* 309.7 and 314.6 eV for RhO_x/CSC, ascribable to Rh3d_{5/2} and Rh3d_{3/2} binding energies of Rh³⁺; after being reduced by H₂, two peaks shift to 308.8 and 313.7 eV, assigned to two spin splitting Rh3d_{5/2} and Rh3d_{3/2} peaks of Rh⁰ metal.

Ranade reported that there were tetrahedrally and octahedrally coordinated Ni²⁺ species on the supported Ni samples,⁴⁶ in which the former was less reducible than the latter. Fig. 6 shows the H₂-TPR profiles of the supported Ni catalysts, in which the reduction peaks of nickel species appear in the range

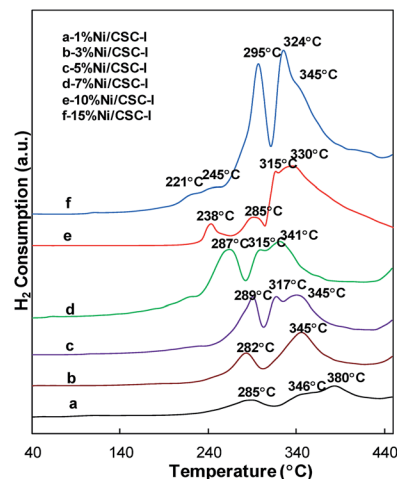


Fig. 6 Effect of Ni content on H₂-TPR profiles of NiO/CSC.

of 200–400 °C. The nickel species reduced at low temperature is attributed to NiO dispersed on the support;⁴³ however, those reduced at high temperature can be assigned to NiO interacted strongly with the support, which will form a few surface layers of the support–NiO complexes.⁴⁷ The presence of Ni²⁺ in the sample can be excluded by the absence of the reduction peak at around 200 °C,⁴⁸ in agreement with the XPS result. Thus, in the TPR profile of 10% Ni/CSC four TPR signals at 238, 285, 315 and 330 °C are ascribable to the reduction of NiO particles to metal Ni⁰ without interaction with the support (at 238, 285 and 315 °C), and to the reduction of Ni²⁺ with medium interaction (at 330 °C). The H₂ consumption peak for the formation of Ni/CSC with different Ni loadings in the range of 3–10% is very similar. There is a new TPR reduction peak for the resulting 1% Ni/CSC at high temperature of 380 °C, with the appearance of other two peaks at 285 and 346 °C, attributable to the reduction of Ni²⁺ with strong interaction. The H₂-TPR profile of 15% Ni/CSC shows that the reduction of nickel species on CSC occurs in five stages with maximal signals at 221, 245, 295, 324 and 345 °C, in which the first reduction peak appears at lower temperature than the former five samples.

Similarly, the H₂-TPR tests are conducted to monitor the reduction behaviors of other metal oxides on CSC (calcined at 400 °C). As shown in Fig. S5,[†] there is no obvious H₂ consumption peak for 10% Mo/CSC at the temperature lower than 440 °C. Even if at 450 °C, molybdenum in the catalyst still exists in the form of oxides. This means the difficult reduction of MoO_x at low temperature. Three weak peaks at 173, 242 and 355 °C can be observed in the TPR profile of the 10% Fe/CSC sample, attributable to the conversion of Fe₂O₃ to Fe₃O₄. For CoO_x/CSC, there are three reduction peaks, in which the TPR peaks from 283 to 377 °C belong to the reduction of CoO_x to Co⁰ metal, and those from 229 to 283 °C correspond to the reduction of Cu²⁺ having weak interaction with the support.

3.2. Catalytic one-step hydrogenation of NB to CHA

3.2.1. Catalytic activity of the supported metal catalysts. As shown in Fig. 7, the catalytic activity of several Rh/CSC catalysts

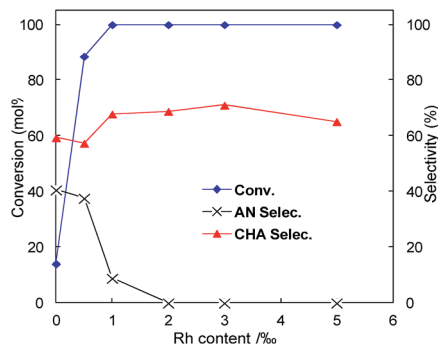


Fig. 7 Catalytic activity of the supported Rh catalysts. (Conditions: catalyst amount, 100 mg; NB, 1 g; LiOH, 40 mg; solvent, THF 9 g; pressure, 3.5 MPa H₂; temperature, 140 °C; time, 6 h).

for the catalytic hydrogenation of nitrobenzene (NB) has been tested in THF at 140 °C. Under mild conditions, different catalysts with different Rh contents show a great difference in the catalytic synthesis of cyclohexylamine (CHA). When only the support CSC is added, only 14.1 mol% of NB is converted with 54.4% selectivity of CHA. The use of 0.5% Rh/CSC as the catalyst increases the conversion of NB to 88.6 mol%, with only 57.4% selectivity of CHA. Evidently, the catalytic activity of 0.5% Rh/CSC catalysts is greatly enhanced, significantly better than that of CSC. From Fig. 7, we can see that 3% Rh/CSC achieves 100 mol% conversion of NB and the highest selectivity of CHA (71.1%) under the same reaction conditions. The catalytic activity can be arranged in the order of 1% Rh/CSC = 2% Rh/CSC = 3% Rh/CSC = 5% Rh/CSC > 0.5% Rh/CSC > CSC, slightly different from the descending order of the CHA selectivity: 3% Rh/CSC > 2% Rh/CSC > 1% Rh/CSC > 5% Rh/CSC > 0.5% Rh/CSC > CSC.

The loading amount of nickel has a great impact on the performance of the catalyst.^{49–51} The effect of the Ni loading on Ni/CSC has been carefully investigated and presented in Table 1. When 1 wt% Ni is loaded on CSC, the conversion of NB is only 34.4 mol%. As the Ni content is increased from 3 to 7 wt%, the conversion of NB is largely improved from 56.2 to 100 mol%. With a continuous increase of the Ni loading from 10 to 15 wt%, the conversion of NB is maintained at 100 mol%. The selectivity for CHA is reduced in the descending order of

Table 1 Catalytic activity of the supported Ni catalysts^a

Catalysts	Conversion (mol%)	Selectivity (%)		
		AN	CHA	Others
1% Ni/CSC	34.4	91.9	8.1	0
3% Ni/CSC	56.2	86.7	11.0	2.3
5% Ni/CSC	89.3	65.1	2.7	5.2
7% Ni/CSC	100	52.8	42.1	5.1
10% Ni/CSC	100	29.0	64.4	6.6
15% Ni/CSC	100	24.5	62.1	13.4

^a Conditions: catalyst amount, 100 mg; NB, 1 g; LiOH, 40 mg; solvent, THF 9 g; pressure, 3.5 MPa H₂; temperature, 140 °C; time, 6 h.

64.4% (10% Ni) > 62.1% (15% Ni) > 42.1% (5% Ni) > 11.1% (3% Ni) > 8.1% (1% Ni). The literature has disclosed the activity dependence of the catalytic hydrogenation of aromatic rings on the particle size of the supported metals.⁵² However, in the present study it is difficult to distinguish the effect of the particle size from the Ni content, because the high loading has led to a large quantity of easily reducible NiO species, and a number of active metal Ni sites on the support, beneficial to the hydrogenation of aromatic rings.

However, once CSC supported Ni and less Rh composite catalyst is prepared, the catalytic activity and the selectivity of CHA are notably improved, as listed in Table 2. The catalytic activity of Rh–Ni/CSC is higher than those of Rh/CSC and Ni/CSC catalysts. On all the Rh–Ni/CSC composite catalysts, the conversion of NB has reached 100 mol%, but the selectivity of CHA shows a descending order of 3% Rh–10% Ni/CSC (91.6%) > 3% Rh–7% Ni/CSC (88.4%) > 3% Rh–5% Ni/CSC (85.9%) > 5% Rh–10% Ni/CSC (84.8%) > 3% Rh–15% Ni/CSC (82.9%) > 3% Rh–3% Ni/CSC (80.9%) > 3% Rh–1% Ni/CSC (80.0%) > 2% Rh–10% Ni/CSC (73.8%) > 1% Rh–10% Ni/CSC (70.9%) > 0.5% Rh–10% Ni/CSC (67.4%). For the titled reaction, 3% Rh–10% Ni/CSC is the most active and selective.

As shown in Table S2,† among various Rh–M/CSC composite catalysts, only 3% Rh–10% Ni/CSC exhibits the best catalytic performance, possibly attributed to the effectiveness of Ni and Rh for catalyzing the titled hydrogenation. All other Rh–M/CSC catalysts can convert 100 mol% NB, but the selectivity of CHA is lower than 52.9%. Clearly, over 10% Cu/CSC, 10% Co/CSC, 10% Fe/CSC and 10% Mo/CSC the partially-hydrogenated product aniline is dominant, while the selectivity of fully-hydrogenated product CHA is extremely low <2.2%. Over these Rh–M/CSC catalysts, the selectivity of CHA exhibits a descending order of 3% Rh–10% Ni/CSC (91.6%) > 3% Rh–10% Cu/CSC (52.9%) > 3% Rh–10% Co/CSC (41.1%) > 3% Rh–10% Mo/CSC (34.6%) > 3% Rh–10% Fe/CSC (25.3%).

3.2.2. Effect of various reaction conditions. Based on the above results, the catalyst 3% Rh–10% Ni/CSC exhibits the best activity for the full hydrogenation of NB to CHA, so it is used to study the effect of various reaction conditions. Under identical

Table 2 Catalytic activity of Ni–Rh/CSC composite catalysts^a

Catalysts	Conversion (mol%)	Selectivity (%)		
		AN	CHA	Others
3% Rh–1% Ni/CSC	100	10.0	80.0	9.1
3% Rh–3% Ni/CSC	100	9.5	80.9	10.5
3% Rh–5% Ni/CSC	100	7.0	85.9	7.1
3% Rh–7% Ni/CSC	100	3.0	88.4	8.6
3% Rh–10% Ni/CSC	100	0	91.6	8.4
3% Rh–15% Ni/CSC	100	7.3	82.9	6.7
0.5% Rh–10% Ni/CSC	100	29.6	67.4	3.0
1% Rh–10% Ni/CSC	100	26.2	70.9	2.9
2% Rh–10% Ni/CSC	100	22.1	73.8	4.0
5% Rh–10% Ni/CSC	100	0	84.8	15.2

^a Conditions: catalyst amount, 100 mg; NB, 1 g; LiOH, 40 mg; solvent, THF 9 g; pressure, 3.5 MPa H₂; temperature, 140 °C; time, 6 h.

experimental conditions, different carriers show different catalytic activities for the catalytic hydrogenation of NB to CHA, especially for the selectivity of CHA (in Table 3). For the CSC supported Rh catalysts, the catalyst 3% Rh/CSC exhibits the highest CHA selectivity of 71.1%. When AC (activated carbon) and G (graphite) are used as the catalyst carriers, 52.3% of the CHA selectivity over 3% Rh/AC is higher than 43.3% over 3% Rh/G. For the supported Rh–Ni composite catalysts, the selectivity of CHA reduces in a sequence of 91.6% over 3% Rh–10% Ni/CSC > 71.5% over 3% Rh–10% Ni/AC > 70.8% over 3% Rh–10% Ni/G.

Four kinds of basic additives such as LiOH, NaNH₂, K₂CO₃ and NaHCO₃, have been tested in the process of hydrogenation. The basic additives can neutralize the surface acidic sites and thus prevent amine intermediates from the strong adsorption on the support, leading to an increase in the CHA selectivity.⁵³ Moreover, the addition of additives can suppress the occurrence of cracked reactions during the hydrogenation, but decrease the catalytic activity as well.⁵⁴ As listed in Table S3,† the basic additives promote the selective production of CHA. Especially, the catalyst 3% Rh–10% Ni/CSC can obtain the highest selectivity of CHA (91.6%) in the presence of LiOH. However, the addition of NaNH₂, K₂CO₃ or NaHCO₃ decreases the selectivity of CHA. The effect of LiOH additive on the hydrogenation of NB is shown in Fig. 8. When no LiOH is added, 100 mol% of NB is converted with only 53.3% selectivity of CHA. When the amount

of LiOH is increased from 10 to 40 mg, the conversion of NB is still kept at 100 mol%, accompanied by the increase of the CHA selectivity from 78.2 to 91.6%. As the amount of LiOH is added to 50 mg, the selectivity of CHA is slightly reduced to 91.0%. Apparently, the addition of LiOH reduces the occurrence of side reactions, beneficial to the enhancement of the CHA selectivity. Consequently, one possible reason for the enhanced selectivity is that the addition of LiOH suppresses the acidity of the catalyst, limiting the occurrence of condensation reactions.⁵⁵

As we have known, the solvent plays a key role in determining the reaction rate or the distribution of products. Various solvents have been applied in the hydrogenation reaction of NB to CHA over 3% Rh–10% Ni/CSC catalyst (Table 4). The tested solvents include THF, cyclohexane, dioxane, ethyl acetate, toluene and cyclohexanol. When these solvents are used, the conversion of NB reaches 100 mol%; however, the selectivity of CHA decrease in the order of THF (91.6%) > cyclohexane (87.6%) > ethyl acetate (56.8%) > cyclohexanol (47.5%) > toluene (33.2%) > dioxane (27.7%). It seems that THF is preferred for the full hydrogenation of nitrobenzene to CHA.

The effect of reaction temperature on the hydrogenation of NB with H₂ over 3% Rh–10% Ni/CSC catalyst is studied, as illustrated in Fig. S6.† As the reaction temperature is increased from 110 to 120 °C, the conversion of NB is increased from 85.2 to 100 mol%. At reaction temperatures above 120 °C, the NB conversion of 100 mol% is maintained. The selectivity for CHA is only 52.4% at 110 °C, which is rapidly increased to 86.5% at 120 °C and 90.1% at 130 °C, gradually to the maximum of 91.6% at 140 °C, and then slightly reduced to 89.2% at 150 °C and 84.3% at 170 °C. Fig. S7† exhibits the effect of reaction time on the hydrogenation of NB over 3% Rh–10% Ni/CSC at 140 °C. Within the reaction time of 1 h, the conversion of NB is about 89.2 mol%, which is rapidly increased to 100 mol% in 2 h. As the reaction time is prolonged to 4, 6 or 8 h, the conversion of NB has been kept at 100 mol%. The selectivity of fully-hydrogenated product (CHA) is lower than 61% within 2 h, which is rapidly increased to 80.1% in 4 h, and to the maximum of 91.6% in 6 h, and then slightly decreased to 87.2% in 8 h.

In the catalytic hydrogenation reaction, the hydrogen pressure is a very important parameter, as hydrogen is one of the reactants. Fig. S8† shows the effect of hydrogen pressure on the conversion of NB over 3% Rh–10% Ni/CSC at 140 °C.

Table 3 Effect of carriers on the hydrogenation^a

Catalysts	Conversion (mol%)	Selectivity (%)		
		AN	CHA	Others
3% Rh/CSC	100	0	71.1	28.9
3% Rh–10% Ni/CSC	100	0	91.6	8.4
3% Rh/AC	100	0	52.3	47.7
3% Rh–10% Ni/AC	100	20.2	71.5	8.3
3% Rh/G	100	16.1	43.3	40.6
3% Rh–10% Ni/G	100	23.7	70.8	5.5

^a Conditions: NB, 1 g; catalyst, 100 mg; LiOH, 40 mg; solvent, THF 9 g; pressure, 3.5 MPa H₂; temperature, 140 °C; time, 6 h.

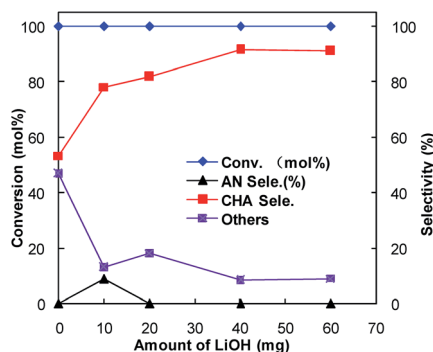


Fig. 8 Effect of LiOH amount on the hydrogenation. (Conditions: catalyst, 3% Rh–10% Ni/CSC 100 mg; NB, 1 g; solvent, THF 9 g; pressure, 3.5 MPa H₂; temperature, 140 °C; time, 6 h).

Table 4 Effect of solvents on the hydrogenation^a

Catalysts	Solvent	Conversion (mol%)	Selectivity (%)		
			AN	CHA	Others
3% Rh–10% Ni/CSC	THF	100	0	71.1	28.9
	Cyclohexane	100	0	91.6	8.4
	Dioxane	100	0	52.3	47.7
	Ethyl acetate	100	20.2	71.5	8.3
	Toluene	100	16.1	43.3	40.6
	Cyclohexanol	100	23.7	70.8	5.5

^a Conditions: catalyst, 3% Rh–10% Ni/CSC 100 mg; NB, 1 g; LiOH, 40 mg; solvent, 9 g; pressure, 3.5 MPa H₂; temperature, 140 °C; time, 6 h.

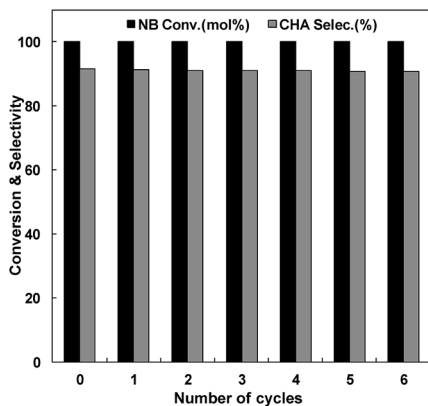


Fig. 9 Recycling results of the catalyst 3% Rh-10% Ni/CSC. (Conditions: solvent, THF 9 g; pressure, 3.5 MPa H₂; temperature, 140 °C; time, 6 h).

The conversion of NB is 90.2 mol% under 2.0 MPa of H₂ pressure, which is increased to 100 mol% at 2.5–4.0 MPa. The selectivity of CHA is increased from 64.4% (at 2.0 MPa) to the maximum of 91.6% (at 3.5 MPa), and then slightly decreased to 90.2% at 4.0 MPa. Therefore, the most appropriate H₂ pressure is about 3.5 MPa, considerably conducive to the adsorption of reactants on the catalyst surface and thereby the fast occurrence of full-hydrogenation of NB to CHA.⁴⁴ This implies that fully-hydrogenated products can be merely formed under a suitable H₂ pressure. This dependence is in agreement with the observations during the hydrogenation of naphthalene.^{56,57}

3.3. Recycling studies

The recycling experiments of 3% Rh-10% Ni/CSC catalyst for the hydrogenation of NB are conducted. As observed from Fig. 9, the activity of catalyst is still maintained at a high level, even if 3% Rh-10% Ni/CSC has been reused six times. This could be ascribed to the strong interaction of the supported metals with the support as disclosed by the H₂-TPR profiles, further inhibiting the leaching of metallic species during the reaction. The conversion of NB is always kept at 100 mol%, while the selectivity of fully-hydrogenated CHA has kept an inconspicuous fluctuation of around 90.6–91.6%. ICP analyses of the reaction mixture did not detect the leaching of Ni or Rh from 3% Rh-10% Ni/CSC recycled. The structure of the reused catalyst has been characterized by XRD, XPS and TEM, and the corresponding data are shown in the Fig. S9–S11. The XRD patterns, XPS spectra and TEM images testify that the amorphous structure of recovered 3% Rh-10% Ni/CSC is still retained even if it has been reused 5 times. This study further reveals the recyclable stability of the active catalyst 3% Rh-10% Ni/CSC for the hydrogenation reaction of NB.

3.4. Catalytic hydrogenation of other substituted nitrobenzenes

Aside from the catalytic hydrogenation of NB with H₂ as stated above, that of other six substituted nitrobenzenes over 3%

Table 5 The hydrogenation results of other substituted nitrobenzenes^d

Catalysts	Solvent	Conversion (mol%)	Selectivity (%)		
			Partial	Full	Others
3% Rh-10% Ni/CSC		100	0	91.6	8.4
		100	0	89.6	10.4
		100	0	94.4	5.6
		100	3.0	80.0	17.0 (14.8) ^b
		100	2.3	75.6	22.1 (19.9) ^c
		100	3.4	76.7	19.9 (17.2) ^d
		100	3.2	72.9	23.9 (20.1) ^e

^a Conditions: catalyst, 3% Rh-10% Ni/CSC 100 mg; substrate, 1 g; LiOH, 40 mg; solvent, THF 9 g; pressure, 3.5 MPa H₂; temperature, 140 °C; time, 6 h. ^b 4,4'-Dimethyl-dicyclohexylamine 14.8%. ^c Cyclohexylamine 19.9%. ^d Cyclohexylamine 17.2%. ^e Cyclohexylamine 20.1%.

Rh-10% Ni/CSC is as well described in Table 5. Comparatively, the conversion of these substituted nitrobenzenes reaches 100 mol%, totally different from the descending order of the selectivity of fully-hydrogenated products: 3-methyl NB (94.4%) > NB (91.6%) > 2-nitrotoluene (89.6%) > 4-methyl NB (80.0%) > 3-chloro NB (76.7%) > 2-chloro NB (75.6%) > 4-chloro NB (72.9%). For chloro-substituted nitrobenzene compounds, the selectivity of fully-hydrogenated products is lower than that of CHA, possibly relevant to the occurrence of partially-dechlorinated reaction during the hydrogenation process, for which some dechlorinated products have been detected by GC-MS.

4. Conclusion

This work reports highly selective 'one-step' liquid-phase hydrogenation of nitrobenzene with nitro group and aromatic ring to cyclohexylamine over the supported 10% Ni/CSC catalysts doped with 3% Rh. Under optimal conditions, almost 100 mol% conversion of the substrate is obtained over 3% Rh-10% Ni/CSC catalyst with a high selectivity of cyclohexylamine up to 91.6%, notably higher than 30–50% selectivity in industrial processes. Some factors affecting the reaction are revealed through conducting a number of reactions and wide characterizations. The addition of alkaline LiOH as an additive limits the occurrence of side reactions, beneficial to the enhancement of full hydrogenation. The XPS results suggest that there is a net transfer of electrons towards Rh-Ni to increase the binding energies of Ni2p and Rh3d once NiO-RhO_x oxides are reduced to metallic Rh-Ni with H₂. The H₂-TPR temperatures of different samples are different from one another, which affects the catalytic activity. The recycling tests reveal recyclable stability of 3% Rh-10% Ni/CSC catalyst.

Acknowledgements

The authors thank the financial supports by National Natural Science Foundation of China (21173073, 21273064, 21503074, 21571055), by the Natural Science Fund for Creative Research Groups of Hubei Province of China (2014CFA015), and by the 2014 Sci-tech Support Project of the Science and Technology Department of Hubei Province of China (2014BAA098).

References

- 1 B. H. Cooper and B. B. L. Donnison, *Appl. Catal., A*, 1996, **137**, 203.
- 2 T. C. Huang and B. C. Kang, *Ind. Eng. Chem. Res.*, 1995, **34**, 2349.
- 3 W. Qian, H. Shirai, M. Ifuku, A. Ishihara and T. Kabe, *Energy Fuels*, 2000, **14**, 1205.
- 4 L. Zhou, H. Z. Gu and X. H. Yan, *Catal. Lett.*, 2009, **132**, 16.
- 5 Y. N. Wang, Y. X. Yang, Y. W. Li, J. H. Lai and K. P. Sun, *Catal. Commun.*, 2012, **19**, 110.
- 6 G. Zhang, L. G. Wang, K. H. Shen, D. F. Zhao and H. S. Freeman, *Chem. Eng. J.*, 2008, **141**, 368.
- 7 X. L. Yang and H. F. Liu, *Appl. Catal., A*, 1997, **164**, 197.
- 8 G. Debus and J. C. Ungers, *Bull. Soc. Chim. Belg.*, 1953, **62**, 172.
- 9 H. G. Liao, Y. J. Xiao, H. K. Zhang, P. L. Liu, K. Y. You, C. Wei and H. A. Luo, *Catal. Commun.*, 2012, **19**, 80.
- 10 X. D. Wang, N. Perret and M. A. Keane, *Appl. Catal., A*, 2013, **467**, 575.
- 11 V. Vishwanathan, S. M. Sajjad and S. Narayanan, *Indian J. Chem., Sect. A: Inorg., Bio-inorg., Phys., Theor. Anal. Chem.*, 1991, **30**, 679.
- 12 S. Narayanan, R. Unnikrishnan and V. Vishwanathan, *Appl. Catal., A*, 1995, **129**, 9.
- 13 G. Mink and L. Horvath, *React. Kinet. Catal. Lett.*, 1998, **65**, 59.
- 14 X. Cui, F. Shi and Y. Deng, *ChemCatChem*, 2012, **4**, 333.
- 15 X. Meng, H. Cheng, Y. Akiyama, Y. Hao, W. Qiao, Y. Yu, F. Zhao, S. I. Fujita and M. Arai, *J. Catal.*, 2009, **264**, 1.
- 16 Y. Motoyama, Y. Lee, K. Tsuji, S. H. Yoon, I. Mochida and H. Nagashima, *ChemCatChem*, 2011, **3**, 1578.
- 17 N. Sakai, K. Fujii, S. Nabeshima, R. Ikeda and T. Konakahara, *Chem. Commun.*, 2010, **46**, 3173.
- 18 J. Skupińska and G. Smółka, *React. Kinet. Catal. Lett.*, 1998, **63**, 313.
- 19 J. Wisniak and M. Klein, *Ind. Eng. Chem. Prod. Res. Dev.*, 1984, **23**, 44.
- 20 F. Zhao, R. Zhang, M. Chatterjee, Y. Ikushima and M. Arai, *Adv. Synth. Catal.*, 2004, **346**, 661.
- 21 M. Chatterjee, M. Sato, H. Kawanami, T. Ishizaka, T. Yokoyama and T. Suzuki, *Appl. Catal., A*, 2011, **396**, 186.
- 22 G. Mink and L. Horváth, *React. Kinet. Catal. Lett.*, 1998, **65**, 59.
- 23 H. S. Kim, S. H. Seo, H. Lee, S. D. Lee, Y. S. Kwon and I. M. Lee, *J. Mol. Catal. A: Chem.*, 1998, **132**, 267.
- 24 S. G. Oh, V. Mishra, J. K. Cho, B. J. Kim, H. S. Kim, Y. W. Suh and Y. J. Kim, *Catal. Commun.*, 2014, **43**, 79.
- 25 H. Greenfield, *J. Org. Chem.*, 1964, **29**, 3082.
- 26 C. F. Winans, *Ind. Eng. Chem.*, 1940, **32**, 1215.
- 27 G. A. Somorjai and Y. Li, *Top. Catal.*, 2010, **53**, 832.
- 28 C. P. Vinod, *Catal. Today*, 2010, **154**, 113.
- 29 E. Schmidt, W. Kleist, F. Krumeich, T. Mallat and A. Baiker, *Chem.–Eur. J.*, 2010, **16**, 2181.
- 30 C. A. Witham, W. Huang, C. K. Tsung, J. N. Kuhn, G. A. Somorjai and F. D. Toste, *Nat. Chem.*, 2010, **2**, 36.
- 31 S. Mostafa, F. Behafarid, J. R. Croy, L. K. Ono, L. Li, J. C. Yang, A. I. Frenkel and B. R. Cuenya, *J. Am. Chem. Soc.*, 2010, **132**, 15714.
- 32 F. Zaera, *Acc. Chem. Res.*, 2009, **42**, 1152.
- 33 P. Maity, C. S. Gopinath, S. Bhaduri and G. K. Lahiri, *Green Chem.*, 2009, **11**, 554.
- 34 S. Diao, W. Qian, G. Luo, F. Wei and Y. Wang, *Appl. Catal., A*, 2005, **286**, 30.
- 35 J. Q. Wang, L. Hu, X. Q. Cao, J. M. Lu, X. M. Li and H. W. Gu, *RSC Adv.*, 2013, **3**, 4899.
- 36 Z. F. Wu and H. Y. Jiang, *RSC Adv.*, 2015, **5**, 34622.
- 37 M. Xie, F. W. Zhang, Y. Long and J. T. Ma, *RSC Adv.*, 2013, **3**, 10329.
- 38 N. M. Patil, M. A. Bhosale and B. M. Bhanage, *RSC Adv.*, 2015, **5**, 86529.
- 39 H. L. Bao, D. S. Wang, X. Y. Wang, C. J. Chen, Y. D. Li and Y. F. Hu, *RSC Adv.*, 2015, **5**, 47125.
- 40 A. Tijani, B. Coq and F. Figuéras, *Appl. Catal.*, 1991, **76**, 255.
- 41 M. H. Liu, W. Y. Yu and H. F. Liu, *J. Mol. Catal. A: Chem.*, 1999, **138**, 295.
- 42 G. M. P. Reinhard Langer, *US Pat.*, 6,054,619 N, 2000.
- 43 X. H. Lu, X. L. Wei, D. Zhou, H. Z. Jiang, Y. W. Sun and Q. H. Xia, *J. Mol. Catal. A: Chem.*, 2015, **396**, 196.
- 44 T. A. Joseph, N. Y. Westbury and J. C. Nils, *US Pat.*, 3,678,108 N, 1972.
- 45 Z. Y. Hou, Q. Yokota, T. Tanaka and T. Yashima, *Appl. Catal., A*, 2003, **253**, 381.
- 46 V. V. Ranade, *Chem. Eng. Sci.*, 1992, **47**, 1857.
- 47 R. Kirumakki Sharath, G. Shpeizer Boris, V. Sagar Guggilla, V. R. Chary Komandur and C. Abraham, *J. Catal.*, 2006, **242**, 319.
- 48 B. Mile, D. Stirling, M. A. Zammitt, A. Lovell and M. Webb, *J. Mol. Catal.*, 1990, **62**, 179.
- 49 R. Kirumakki Sharath, G. Shpeizer Boris, V. Sagar Guggilla, V. R. Chary Komandur and C. Abraham, *J. Catal.*, 2006, **242**, 319.
- 50 S. Mingyong, E. N. Alan and A. John, *J. Catal.*, 2005, **231**, 223.
- 51 A. Saadi, R. Merabti, Z. Rassoul and M. M. Bettahar, *J. Mol. Catal. A: Chem.*, 2006, **253**, 79.
- 52 A. Yu. Stakheev and L. M. Kustov, *Appl. Catal., A*, 1999, **188**, 3.
- 53 Y. Cesteros, R. Fernández, J. Estellé, P. Salagre, F. Medina, J. E. Sueiras and J. L. G. Fierro, *Appl. Catal., A*, 1997, **152**, 249.
- 54 S. Gomez, J. A. Peters and T. Maschmeyer, *Adv. Synth. Catal.*, 2002, **344**, 1037.
- 55 C. Adam, V.-H. Maritza, E. M. Thomas, S. Peter, V. Stan and A. L. Johannes, *J. Catal.*, 2007, **245**, 237.
- 56 S. D. Lin and C. Song, *Catal. Today*, 1996, **31**, 93.
- 57 T. Kotanigawa, M. Yamamoto and T. Yoshida, *Appl. Catal., A*, 1997, **164**, 323.